

NASA CR-177,989

NASA Contractor Report 177989

NASA-CR-177989
19860003113

OPTICAL TECHNIQUE TO STUDY THE IMPACT OF
HEAVY RAIN ON AIRCRAFT PERFORMANCE

Cecil F. Hess and Funming Li

SPECTRON DEVELOPMENT LABORATORIES, INC.
Costa Mesa, California

Contract NAS1-17932
October 1985

FOR REFERENCE

NOT TO BE TAKEN FROM THIS ROOM

LIBRARY COPY

NOV 12 1985

LANGLEY RESEARCH CENTER
LIBRARY, NASA
HAMPTON, VIRGINIA



National Aeronautics and
Space Administration

Langley Research Center
Hampton, Virginia 23665



NF01015

PROJECT SUMMARY

The objective of the research conducted under Phase I is to establish the feasibility of a technique to measure the size and velocity of droplets under heavy rain conditions. Heavy rain, especially accompanied by wind shear, causes many accidents during aircraft landing and take-off. This effect will be quantified in wind tunnel tests at NASA Langley. Necessary measurements for these tests and other related studies are the size and velocity of the droplets, which can be up to seven mm in diameter.

A laser-based technique was investigated and shown to have the potential to obtain the required measurements. A theoretical model was developed which included some simple effects due to droplet nonsphericity. An opto-electronic breadboard was constructed and sprays produced by a BURR 2 nozzle were measured. Parametric studies included the variation of collection distance (up to 4 m), angle of collection, effect of beam interference by the spray, and droplet shape.

Accurate measurements were obtained under extremely high liquid water content and spray interference, using an optical configuration similar to the one required at the NASA wind tunnel.

The technique finds applications in the characterization of two phase flows where the size and velocity of particles are needed. Instruments based on this technique will find application in national laboratories, industry and universities.

TABLE OF CONTENTS

<u>NO.</u>		<u>PAGE</u>
	TABLE OF CONTENTS.....	ii
	LIST OF FIGURES.....	iii
1.0	INTRODUCTION	1
	1.1 Summary of Work Conducted Under Phase I.....	2
2.0	TECHNICAL APPROACH.....	4
	2.1 Description of Technique.....	4
	2.2 Description of Apparatus.....	6
	2.3 Description of Experiments.....	11
	2.4 Calibration Procedure.....	15
3.0	EXPERIMENTAL RESULTS.....	18
	3.1 Characterization of Rain Spray.....	18
	3.2 Spray Interference.....	21
	3.3 Measurements with 4 Mt. Receiving Optics.....	29
4.0	THE EFFECT OF DROPLET ASPHERICITY IN THE SCATTERING SIGNAL.....	30
5.0	REFERENCES.....	38

LIST OF FIGURES

<u>NO.</u>		<u>PAGE</u>
1	Expanded laser sheets of wavelength λ crossing at an angle γ to form an elongated probe volume. Particles move along x as shown.....	5
2	Schematic diagram of Top Hat measurement system.....	7
3	Photograph of a section of the elongated probe volume.....	9
4	Photograph of optical breadboard and particle generation apparatus.....	10
5	Pulse photograph of BORR 2 spray in stagnant air.....	14
6	Size and velocity histograms of 2.8 mm diameter droplets produced by hypodermic needle.....	16
7	Variation of droplet size with probe volume position.....	17
8	Size and velocity histograms of rain spray.....	19
9	Size distribution at the center and edge of rain spray at 60 psi.....	20
10	Size distribution of rain spray.....	22
11	Size histogram of monodisperse spherical droplets illuminated by (a) undisturbed laser beams, (b) laser beams traveling through rain spray.....	24
12	Effect of spray blockage on the data rate of collection as a function of particle size.....	25
13	Doppler signal of spherical droplet illuminated by (a) undisturbed laser beams; (b) laser beams traveling through rain spray. Scale for both pictures 0.1 ms/div and 1v/div.....	27
14	Size distribution of polydisperse spray with and without rain spray interference.....	28
15	Size histogram of monodisperse spherical droplets collected at (a) 20°; (b) 90°.....	31
16	Size histogram of equal volume nonspherical droplets collected at (a) 20°; (b) 90°.....	32
17	(a) Coordinates of ellipsoid; (b) cross section of ellipsoid at $z = 0$; (c) cross section of ellipsoid at $y = 0$ after converting to x'y' coordinates.....	34

1.0 INTRODUCTION

This final report documents the work conducted under Phase I of the SBIR program "Optical Technique to Study the Impact of Heavy Rain on Aircraft Performance."

The feasibility of a technique to measure raindrops under very heavy rain was established, and results are presented.

It has been shown^[1] that heavy rain, especially accompanied by wind shear, is responsible for many accidents during aircraft landing and takeoff. To quantify this effect, wind tunnel measurements will be conducted at NASA Langley to model real situations. The size and velocity of droplets in the free stream are required inputs to these models. Techniques are, therefore, needed to measure very large size droplets (up to seven mm) in very large liquid water content (up to 40 gr/m³) environments.

There are three major problems in characterizing raindrops in heavy rain using optical methods. First, the shape of the natural raindrops may be nonspherical especially for large size droplets.^[2] Since light scattering theories assume for the most part that the droplets are spherical, errors will be incurred when inverting the scattered light information. The selection of optical conditions to minimize this error becomes an important aspect of this work.

In the size range of interest (>100 μm) the scattered light can be divided into three components: diffraction, reflection, and refraction. The first is in the forward direction and cannot be completely separated from the unscattered beam. The last two are more sensitive to shape and must be interpreted carefully. In the simplest case of an

elongated ellipsoid, the scattered light intensity is found to be proportional to the square of its major axis.

Second, the large range of droplet size encountered in heavy rain^[3] can also impose difficulties in the size measurement. In order to measure a particular size range, a suitable size probe volume is required. This probe volume can, however, impose limitations in the number density of smaller droplets.

Finally, beam blockage and interference due to the presence of upstream droplets along the beams can affect the measurements. Beam blockage and interference introduce instantaneous fluctuations to the constant intensity laser beams. These fluctuations not only broaden the size histogram but also reduce the data rate of collection. In this work we designed and constructed an electro-optical breadboard to study the problems listed above and performed measurements of a spray produced by a BURR 2 nozzle. We demonstrated that a laser Top Hat technique can be used to obtain the required measurements. This method based on the absolute scattered light from constant intensity laser beams can measure droplets in the 0.1 mm to 10 mm size range moving at very high speeds.

1.1 Summary of Work Conducted Under Phase I

In this section a brief account of the effort conducted under Phase I is reported. This will provide readers an overview of the program while each section will discuss in detail the various accomplished tasks.

Summary of Tasks

- a) Design and construction of an opto-electronic breadboard. Droplets were illuminated with an almost constant laser intensity profile and size and velocity histograms were obtained.
- b) Implementation of a calibration system using a syringe and hypodermic needle to generate a string of "almost monodisperse" droplets of 2.8 mm in diameter.
- c) Mapping of the optical probe volume. Number density can be calculated from this information and from measured data rate and droplet velocity.
- d) Implementation of a BURR 2 spray nozzle experiment. This nozzle was attached to a 4 m high ceiling and droplets discharging vertically from the nozzle were collected into an aluminum can surrounded with a shower curtain.
- e) Measurement of the liquid water content and the rain fall rate at various water pressures with a single orifice of the nozzle.
- f) Investigation of the effect of beam blockage and interference due to the presence of other droplets in a spray.
- g) Spray measurements with receiver positioned at 4 m from probe volume to simulate the dimensions expected in the wind tunnel.
- h) Investigation of the effect of droplet asphericity on the size measurement. A simple model has been assumed which shows the same trend as the experimental results.

2.0 TECHNICAL APPROACH

The objective of this approach is to measure nonintrusively and in real time the size and velocity of large droplets (few hundred microns to several millimeters) associated with heavy rain. In this section we provide a description of the technique, the apparatus, and the experiments conducted during Phase I.

2.1 Description of Technique

The method studied here bases the size on the amount of light scattered by the individual droplets crossing the probe volume. The velocity is obtained from the classical Doppler signal.

The Gaussian ambiguity is removed by expanding the laser beams with cylindrical lenses and selecting a portion of these expanded beams with a mask. Typically placing a mask in front of a laser beam will produce diffraction rings which will modulate the intensity. To avoid these interference rings and produce a probe volume with a true constant intensity along the plane of the fringes, the mask is imaged on the probe volume. Thus, the intensity distribution across the mask is relayed to the probe volume with the appropriate magnification. Effectively the probe volume is formed by crossing two rectangular beams such that the intensity is (almost) constant along y and Gaussian along x, where x and y are defined in Figure 1.

The intensity distribution at the probe volume is then given by

$$I = 2I_0 \exp\left[-\frac{2}{b^2}(x^2 + z^2 \gamma^2/4)\right] \cdot \left[\cosh\left(\frac{2xz\gamma}{b^2}\right) + \frac{\cos 4\pi x \sin\left(\frac{\gamma}{2}\right)}{\lambda}\right], \quad (1)$$

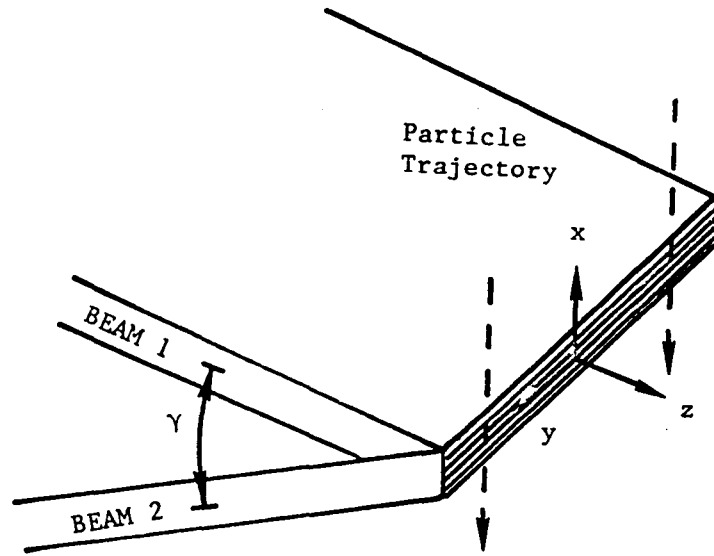


Figure 1. Expanded laser sheets of wavelength λ crossing at an angle γ to form an elongated probe volume. Particles move along x as shown.

where I_0 is the center intensity, b the waist radius, γ the intersection angle, and λ the wavelength. The light scattered from particles crossing this probe volume is given by

$$I_s = IKd^2 \quad , \quad (2)$$

where K is given in Reference [4] for spherical droplets. For a pinhole limited signal $\frac{zy}{2} \approx 0$, therefore, the intensity can be assumed to vary with x only.

The velocity of the droplets is derived from the modulation established by the cosine term of Equation (1).

The size is obtained from the pedestal obtained after low-pass filtering Equation (2).

This pedestal is given by:

$$P = 2 I_0 K_0 d^2 \exp \left(- \frac{2x^2}{b^2} \right) \quad (3)$$

and it is measured by the electronics at $x = 0$.

As will be shown later the droplets may not be spherical, depending on the drag. Therefore, this simple model will be subject to errors. A more complex model which accounts for nonsphericity has been developed and the results are shown in Section 4.0.

2.2 Description of Apparatus

Figure 2 shows a schematic diagram of a Top Hat optical system and the associated electronics. Two cylindrical lenses, L1 and L2,

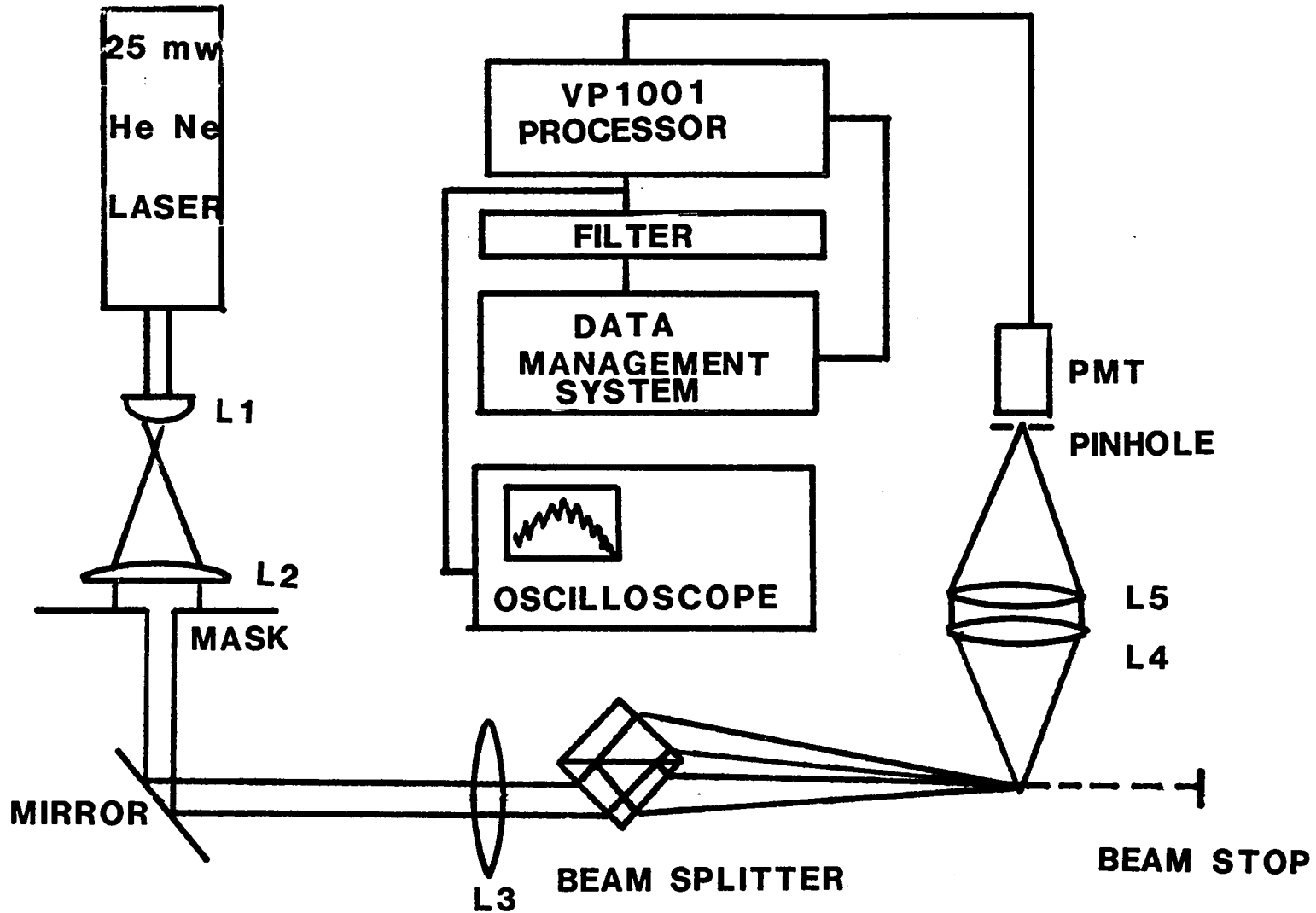


Figure 2. Schematic diagram of Top Hat measurement system.

expand approximately 8 times one dimension of a 1.25 mm diameter He-Ne laser beam. This expanded laser beam was masked with a 3 mm slit placed after the cylindrical lens L2. A spherical lens L3 and a beam splitter were placed such that the mask was imaged at the center of the spray. This was accomplished by placing a tiny hair at the mask and searching for a sharp image at the conjugate plane. The two beams coming out of the beamsplitter were crossed there thus defining the probe volume and interference fringes. Figure 3 shows a photograph of a cross section of the probe volume. F/5 receiving optics placed at 90° imaged the probe volume on a pinhole in front of the PMT thus establishing its length. The output of the PMT was connected to a VP1001 signal processor which was interfaced to a computer. The velocity of the droplets was measured from the Doppler frequency and the size was measured from the peak of the absolute scattered light using a pulse height analyzer interfaced to the frequency counter. A low pass filter eliminated the ac component of the signals measured by the pulse height analyzer.

Size and velocity histograms of the droplets crossing the probe volume were displayed in real time and stored for further analysis. Figure 4 shows a photograph of the optical system and spray experiment. The transmitter and the electronics are on the table at the left. The laser beam is shown turning 90° and illuminating the spray. The receiver is placed on the table at the right.

BEST

AVAILABLE

COPY

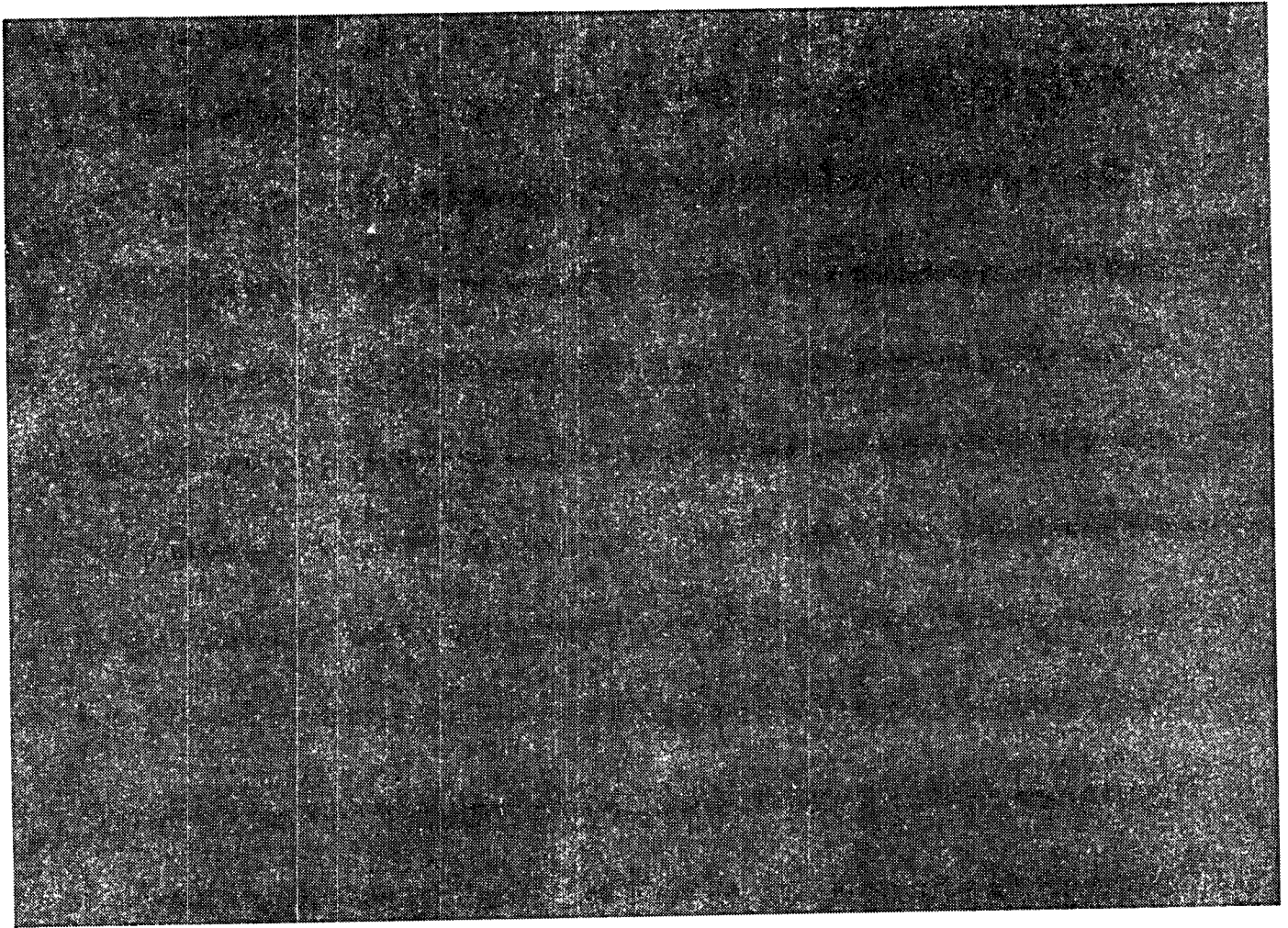


Figure 3. Photograph of a section of the elongated probe volume.

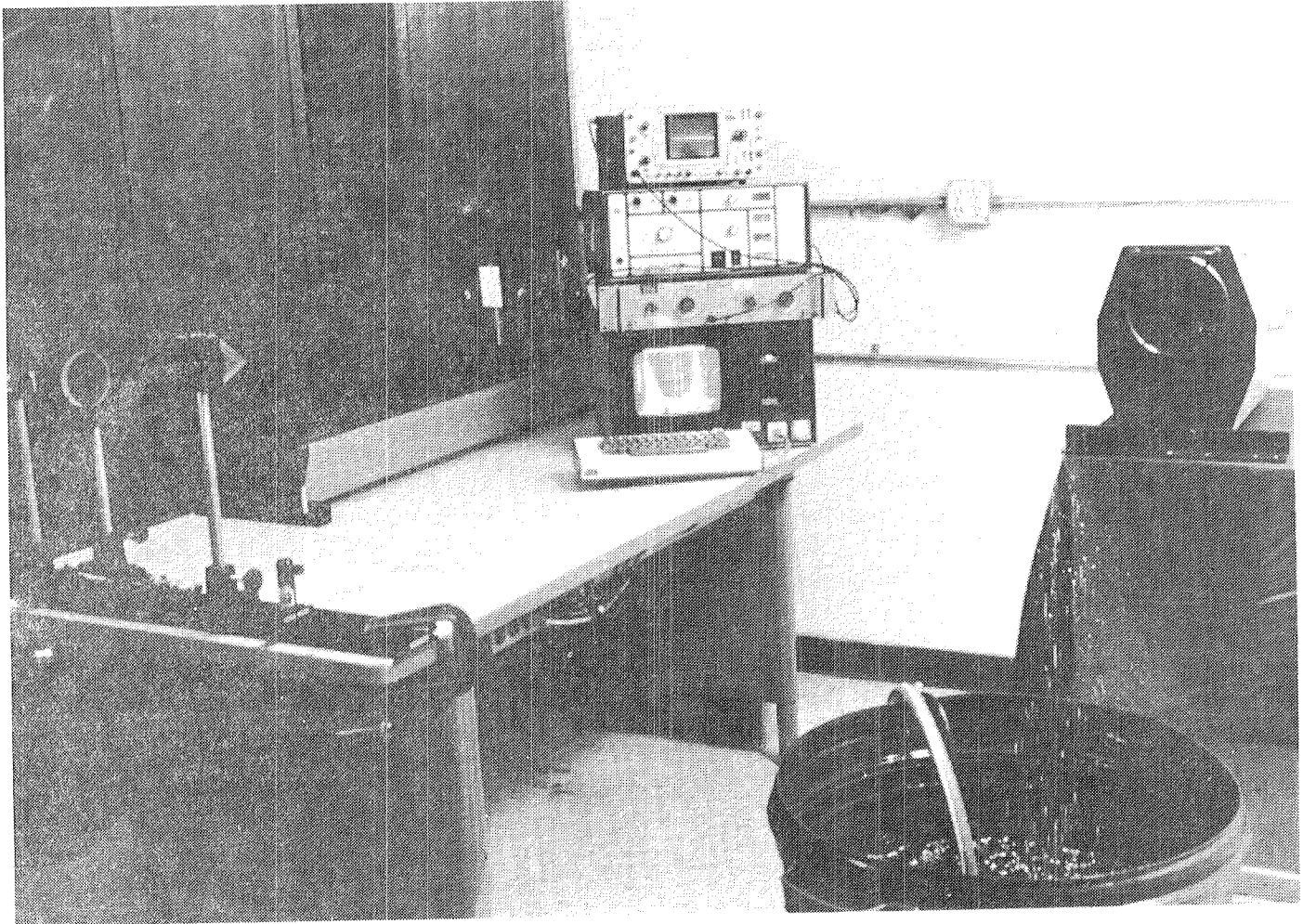


Figure 4. Photograph of optical breadboard and particle generation apparatus.

2.3 Description of Experiments

Three kinds of experiments were conducted to establish the feasibility of the Top Hat technique in measuring heavy rain. These experiments were designed to address the following issues:

- a. The ability to measure a spray produced by a BURR 2 nozzle in the 300 to 9000 μm range.
- b. The effect of spray interference on monodisperse and polydisperse sprays.
- c. The effect of droplet asphericity on the scattered light.

The first type of experiment was conducted using a single orifice of a 5 orifice BURR 2 nozzle. This restriction was imposed by the size of our laboratory which unfortunately is not designed to handle the five orifices at full blast. Visual inspection of the spray indicated that well established droplet regimes existed 2 m from the nozzle tip. We, therefore, installed the nozzle at 4 m from the floor and sprayed down. Measurements were performed at about 2.65 m from the nozzle tip. A pressure gauge next to the nozzle was used to monitor the discharge pressure during measurements. The spray was discharged into a 50 gal. bucket with a submersible pump to dispose of the water. The spray flow rate could be easily established with a stop watch and volume measurement. The optics remained fixed during the experiments and imaged at a predetermined position within the spray.

The effect of spray interference was established by traversing the laser beams through the "rain spray" and forming the probe volume after the spray. At the probe volume we measured monodisperse drops of known size (typically 2.8 mm) or another spray produced by a Spray

Systems pressure nozzle. Typical LWC during the spray measurements and laser interference experiments were about 90 gr/m^3 , which is considerably larger than that encountered under the heaviest of rains.

The liquid water content (LWC) was estimated by measuring the nozzle discharge (\dot{m}), the average droplet velocity (v), and the wet area at the probe volume (A). It is then given by:

$$\text{LWC} = \frac{\dot{m}}{vA} .$$

The mass rate (\dot{m}) was measured volumetrically with a bucket and stopwatch, the wet area (A) was estimated visually, and the velocity of the droplets was measured with LDV.

The rainfall (RR) is related to LWC by the following expression:

$$\text{RR} = \frac{\text{LWC} \times v}{\rho}$$

where ρ is the density of water. Typical LWC and RR values for the single orifice of a BURR 2 nozzle are shown on Table 1. There were two reasons for testing the feasibility of the technique under such large LWC. First, this was the normal level encountered at 3 m from the nozzle tip. Second, we postulated that if we could perform adequate measurements under this heavy particle loading, the technique would most definitely work in the wind tunnel experiments.

The last kind of experiment was to qualify the effect of droplet nonsphericity in the scattered light. Photographs of the spray indicated (Figure 5) that many of the large droplets were nonspherical. The

TABLE 1.

NOZZLE ID : BURR 2 (SINGLE ORIFICE)

WATER PRESSURE (psi)	LIQUID WATER CONTENT (g/m³)	RAIN FALL RATE (cm/hr)
50	81.5	468
60	90.3	521
70	99.3	573

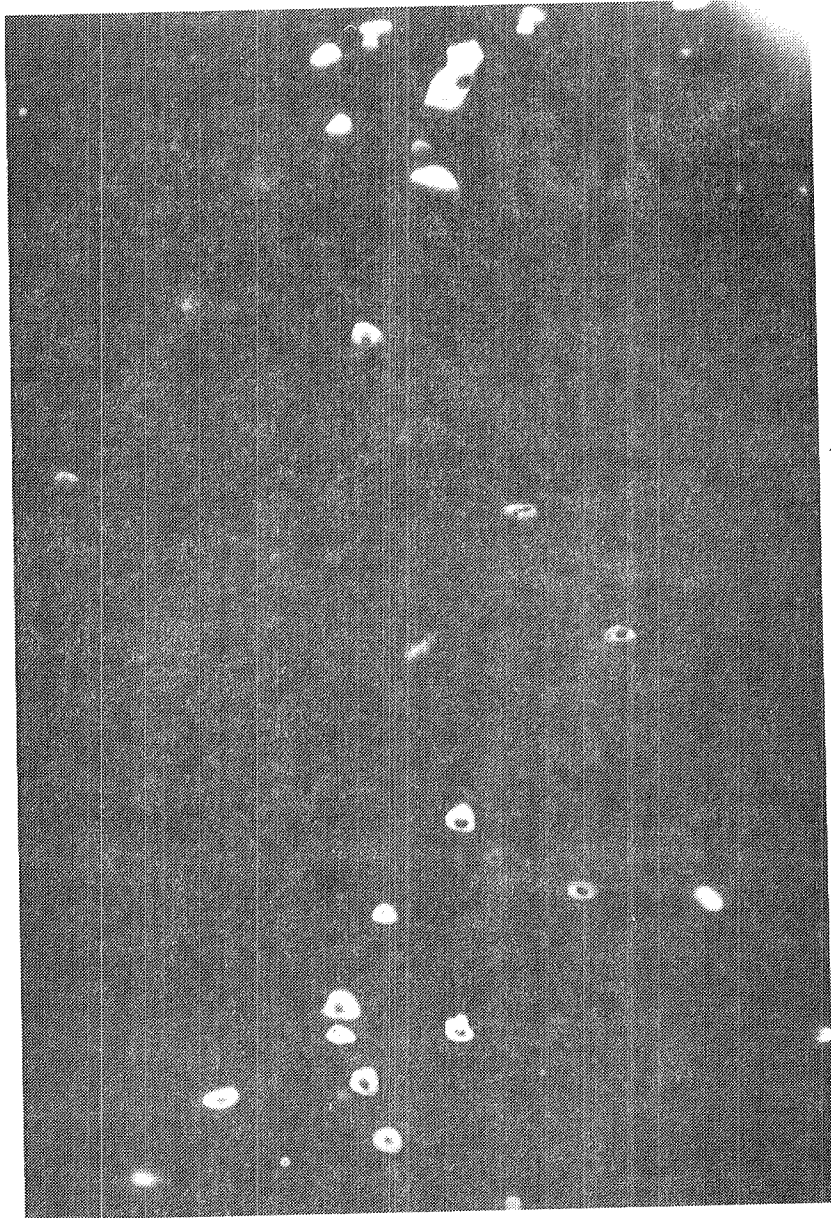


Figure 5. Pulse photograph of BURR 2 spray in stagnant air.

objective of this experiment was to qualify the errors associated with assuming spherical drops. These experiments were conducted with the Berglund-Liu monodisperse droplet generator. Droplets of known volume but aspheric shape were produced with this device.

2.4 Calibration Procedure

A monodisperse string of droplets of 2.8 mm provided the required system calibration. These droplets were produced by allowing water to free fall through a syringe and a hypodermic needle. The size of these droplets was determined by photographic measurements to be $2.8 \text{ mm} \pm 5\%$. The light scattered by the moving droplets was focused onto the PMT of the receiving optics. A mask was placed in front of the collecting lens in order to obtain a visibility-size match for a particular size range of interest. It should be pointed out that the visibility is not part of the size measurement but is required in order to make velocity measurements.

Finally, the gain of the PMT was adjusted manually until the size displayed by the histogram corresponded to the measured drops. Figure 6 shows a representative size and velocity histogram obtained with the 2800 μm calibration drops. These calibration drops were traversed across the probe volume and measured in order to establish the uniformity of the Top Hat profile. Figure 7 shows the relative size as a function of position. The error is less than $\pm 4\%$.

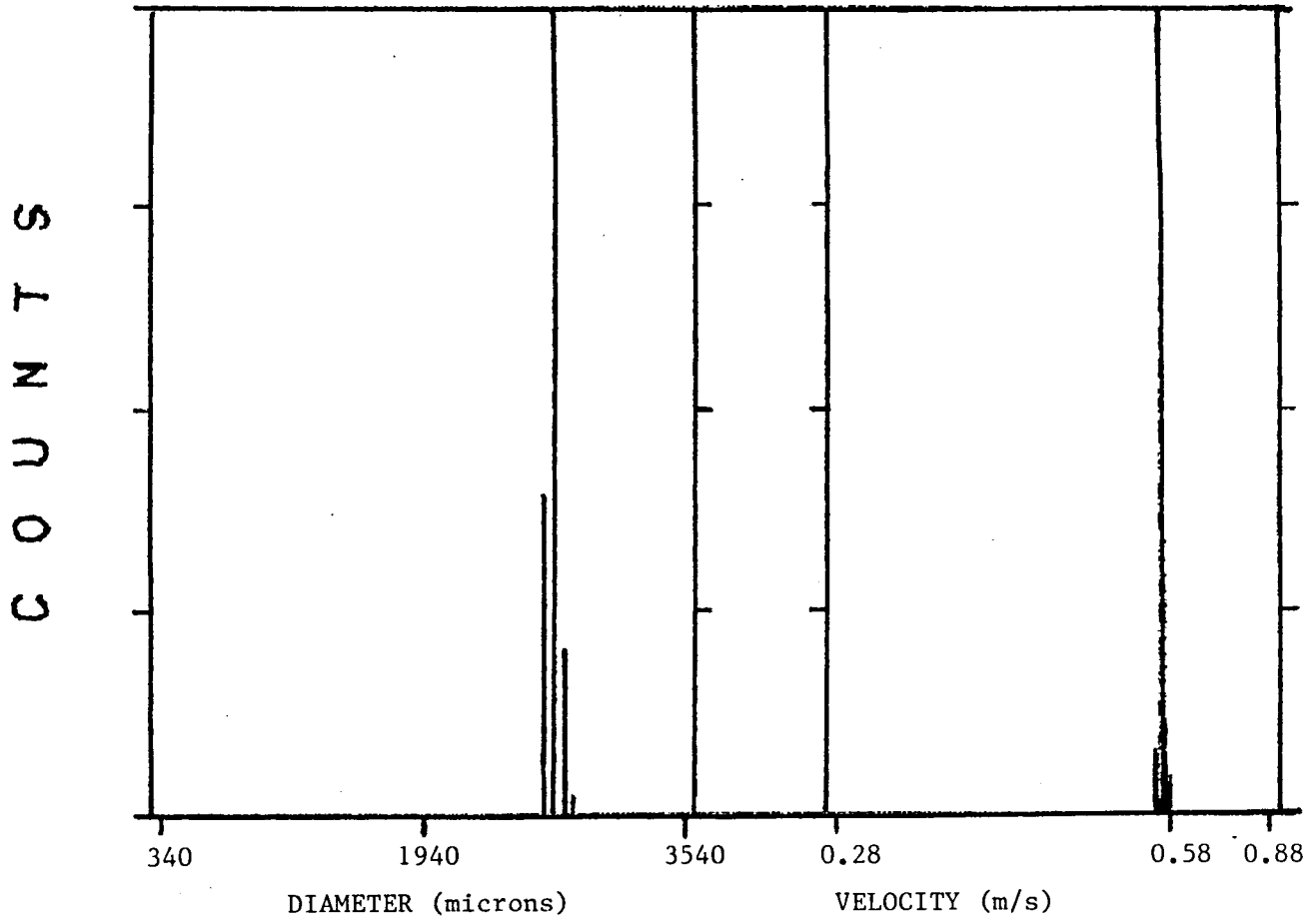


Figure 6. Size and velocity histograms of 2.8 mm diameter droplets produced by hypodermic needle.

VARIATION OF DROPLET SIZE WITH PROBE VOLUME POSITION

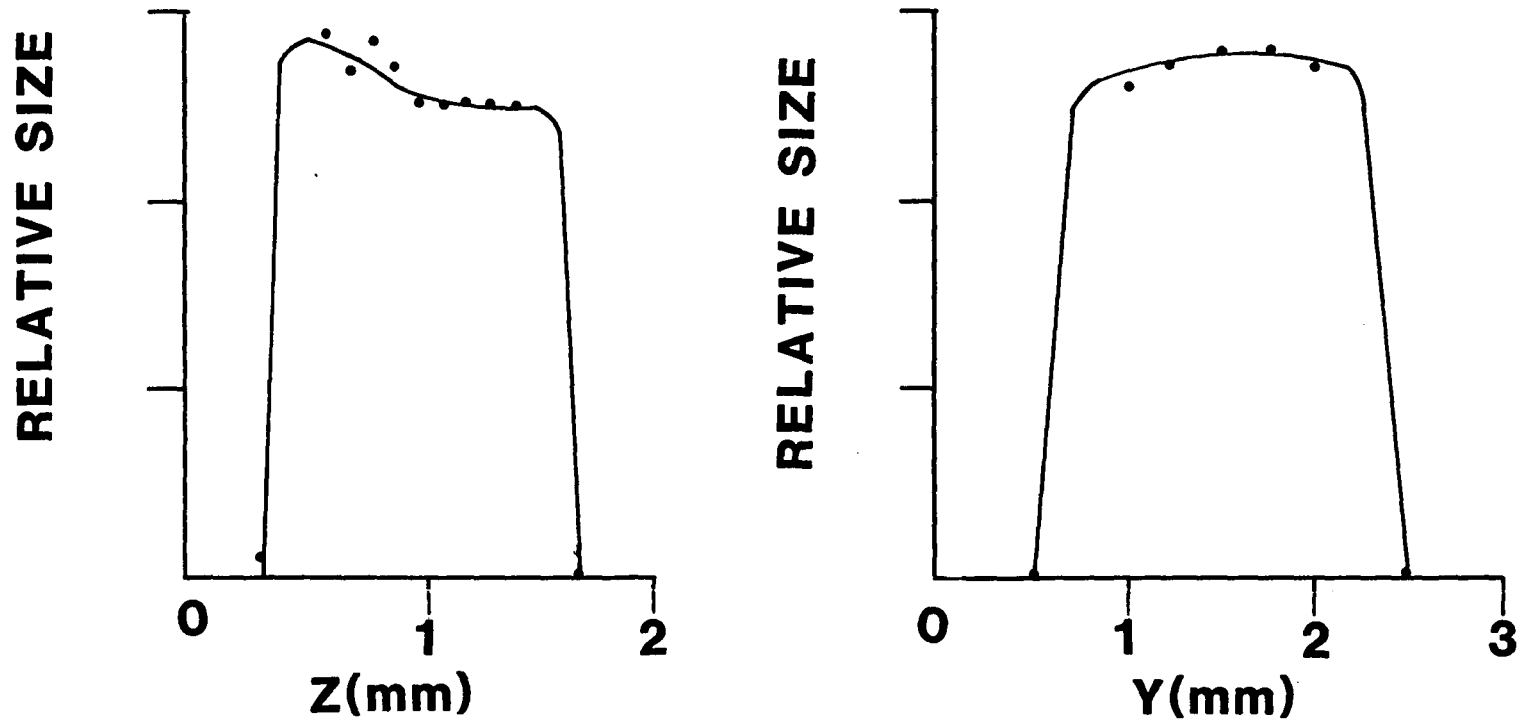


Figure 7.

3.0 EXPERIMENTAL RESULTS

The results of the three kinds of experiments described in the previous section are presented now.

3.1 Characterization of Rain Spray

A rain spray produced by a single orifice of a BURR 2 nozzle was measured at an axial location of 2.65 m from the nozzle tip and two radial locations: $r=0$ and $r=6$ cm. The scattered light was collected at 90° and at 20° , at distances of 0.62 m and 4 m. Most of the measurements were conducted at 0.62 m but some measurements were made at 4 m to simulate wind tunnel dimensions. Nozzle pressures of 50, 60, and 70 psi were investigated.

Typical size and velocity histograms are shown on Figure 8 at $r=0$ for 60 psi. A size range of about 10:1 was imposed by the electronics and to obtain broader size ranges, the measurements were obtained piece-wise.

Figure 9 shows the size distribution corresponding to the center of the spray obtained with three different size ranges. These measurements are plotted together to establish discrepancies in the overlapping regions. The typical trend is that the number of counts is underestimated at the small size end of any range. To some extent this is due to the limited laser power available for this experiment (25 mW HeNe). Also plotted on the same figure is the size distribution corresponding to the edge of the spray. The size range of 100-1000 μm was calibrated with a 283 μm droplet produced by the Berglund-Liu. The measurement cross sectional area was smaller for this case: 0.6 x 2 mm, compared to 1.5 x 2 mm for the other ranges.

pressure=60 psi

radial position= 0

axial position= 2.65m

nozzle ID : BURR 2

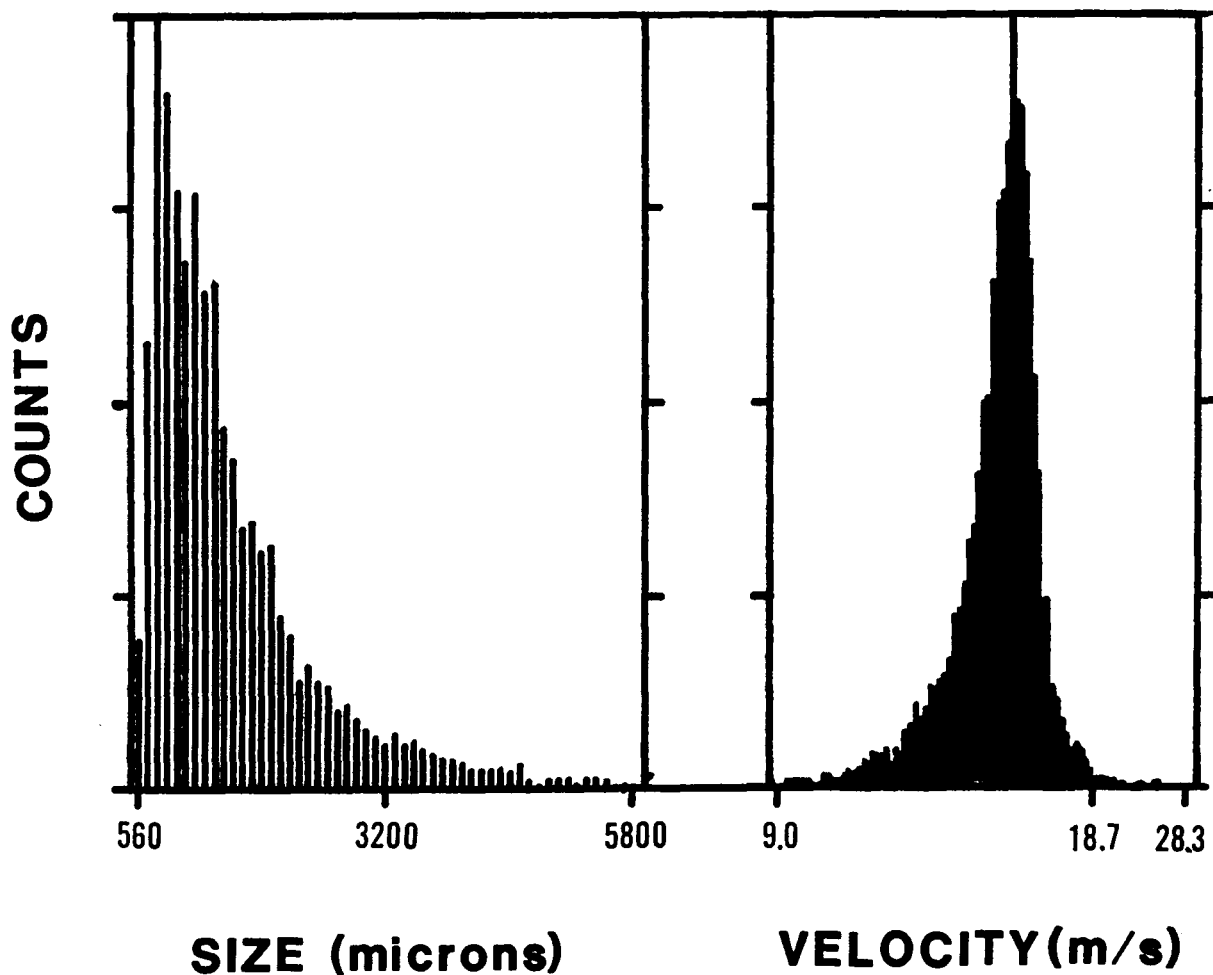
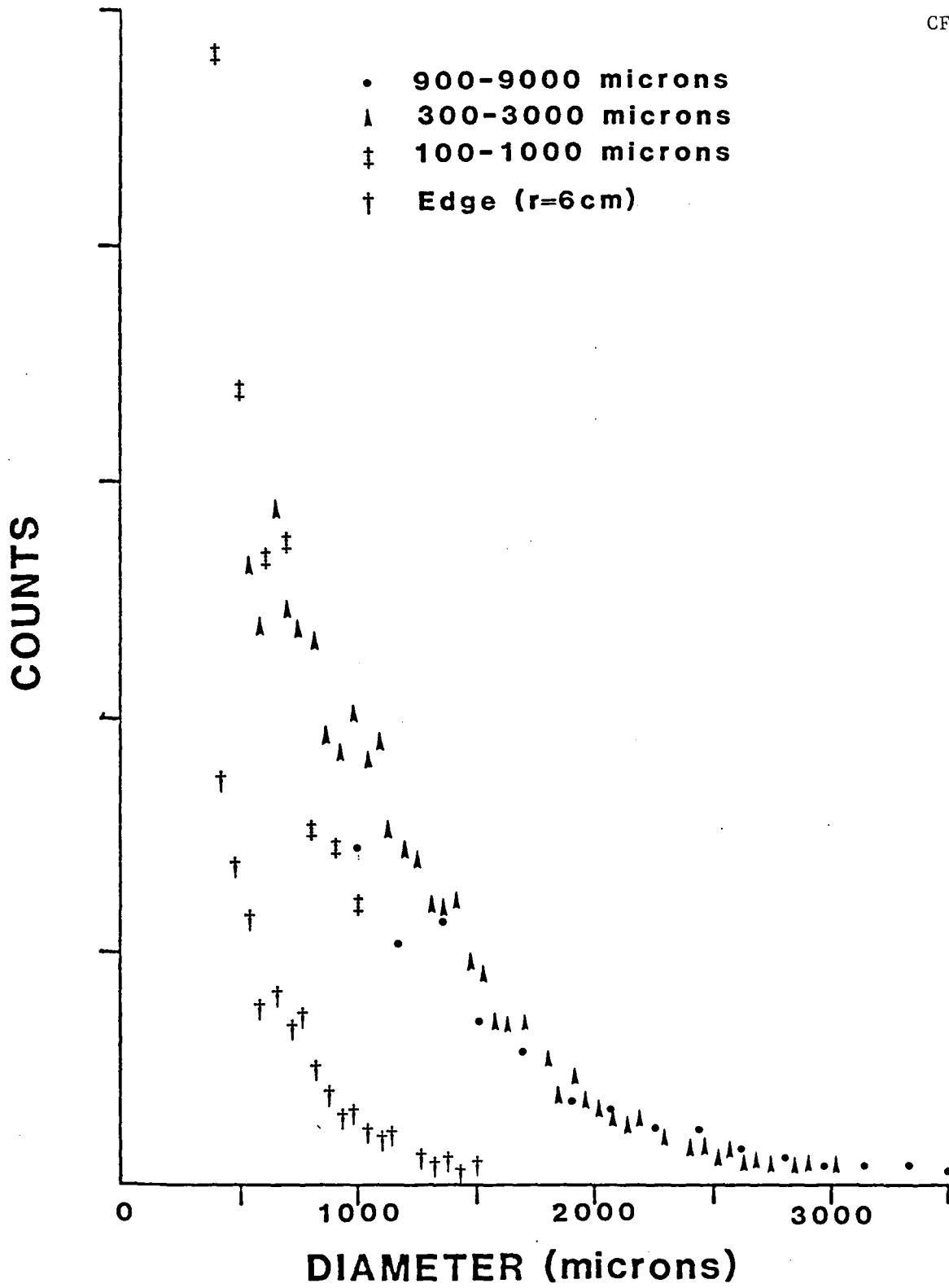


Figure 8. Size and velocity histograms of rain spray.



85-61070

Figure 9. Size distribution at the center and edge of rain spray at 60 psi.

Figures 8 and 9 show that large droplets were produced by the nozzle. Droplets up to 8 mm were measured. The number of droplets was inversely proportional to their volume down to a few hundred microns. Figure 10 illustrates this effect for drops in the 350 μm to 3500 μm range. Obviously these plots would show a different shape if the volume per size class was plotted.

The measurements at the edge of the spray show a lower number density and smaller size distribution, therefore, yielding a smaller Sauter mean and linear mean diameters than those at the center position.

The following table summarizes the results obtained at the center position ($r = 0$) as a function of rain nozzle pressure.

NOZZLE PRESSURE (PSI)	SMD (μm)	LMD (μm)	MEAN VELOCITY (m/s)	PEAK VELOCITY (m/s)
50	1649	1038	13.7 \rightarrow 14.3	15
60	1575	956	14.2 \rightarrow 15.6	16
70	1549	856	14.6 \rightarrow 16.4	17

Keep in mind that these are point measurements and will differ from integrated measurements taken at the same plane.

3.2 Spray Interference

To evaluate the effect of spray interference in the size measurement, monodisperse strings of droplets and polydisperse sprays were measured with and without the heavy rain spray interfering with the

SIZE DISTRIBUTION OF RAIN SPRAY

radial position = 0
axial position = 2.65m
nozzle ID = BURR 2

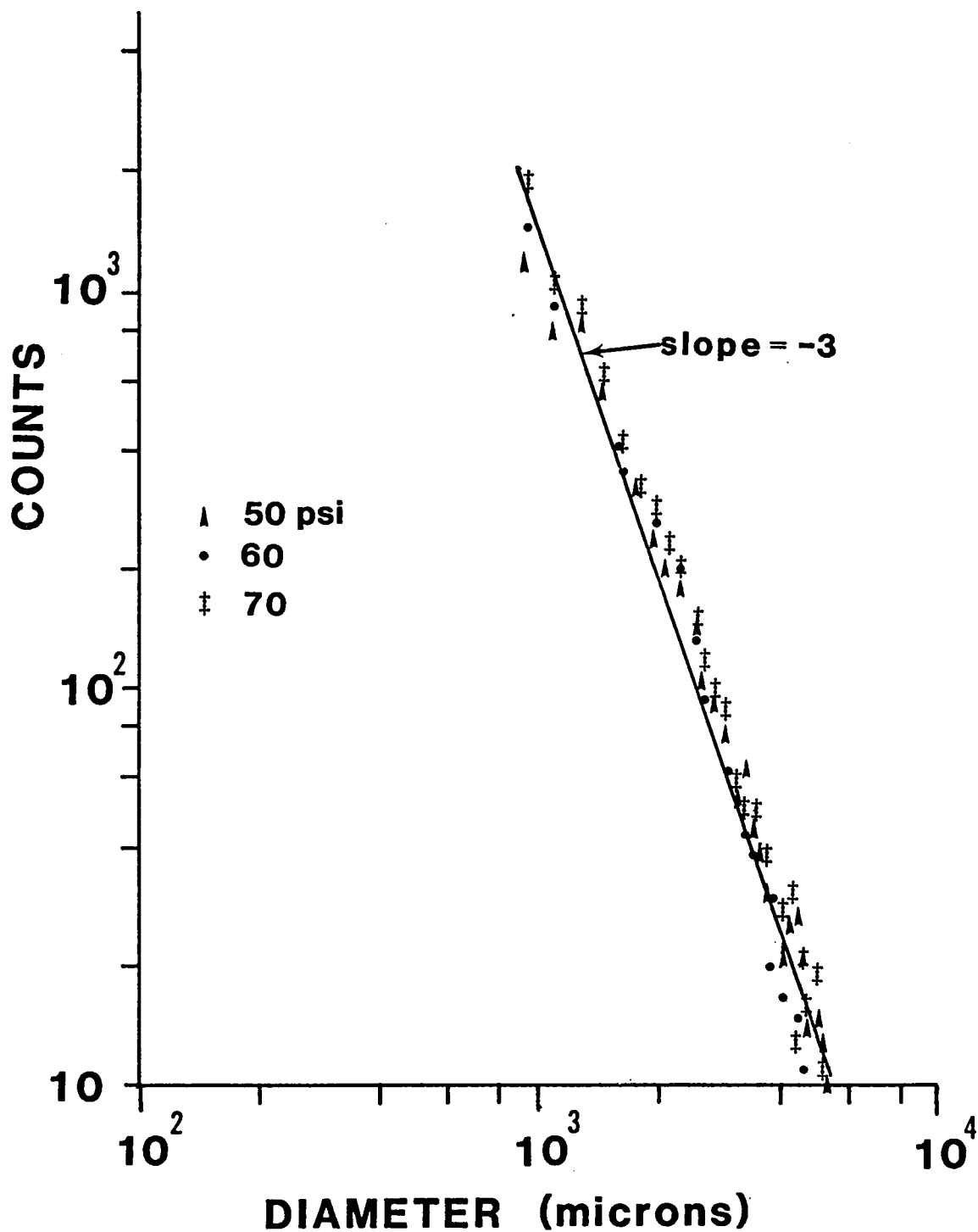


Figure 10.

beams before they crossed to form the probe volume. The results are shown below.

Monodisperse String of Droplets

Droplets of a uniform size were measured with the laser beams traveling through a spray produced by the BURR 2 nozzle. These measurements were compared to those obtained without interference. Since the effect on the size can be a function of the measured size, different size monodisperse droplets were simulated. This simulation was necessary since the droplet generator operated over a very narrow size range centered at 2.8 μm . Different size droplets were then simulated by masking the receiver to obtain the intensity and visibility corresponding to the appropriate size. Figures 11a and 11b, respectively, show the size histograms of a monodisperse string of drops with and without interference. Three effects were observed in these measurements: (1) the mode of the size distribution decreased (from 2739 μm to 2677 μm); (2) the distribution broadened; and (3) the data rate decreased and depended on the particle size. The first effect can be easily attributed to laser obscuration. In many practical situations this effect can be either ignored or compensated for by monitoring the transmitted beam. The second effect can be attributed to the random nature of the spray blockage. In the measurement of a polydisperse spray, this effect will go unnoticed since the broadening between bins will result in almost zero net exchange. The third effect can be more serious and difficult to correct. It is illustrated in Figure 12 where the data rate is plotted as a function of drop size. The trend was

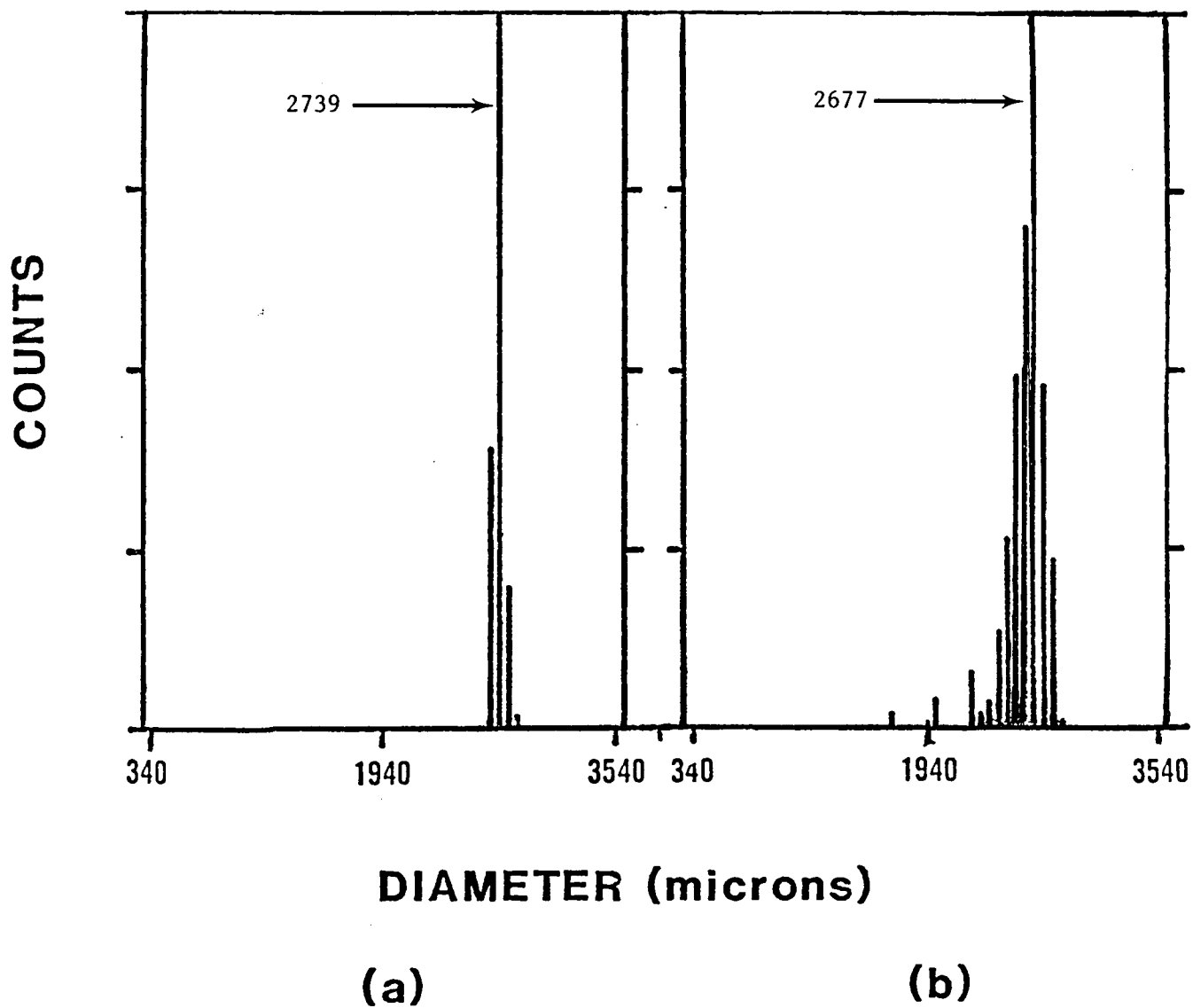


Figure 11. Size histogram of monodisperse spherical droplets illuminated by (a) undisturbed laser beams, (b) laser beams traveling through rain spray.

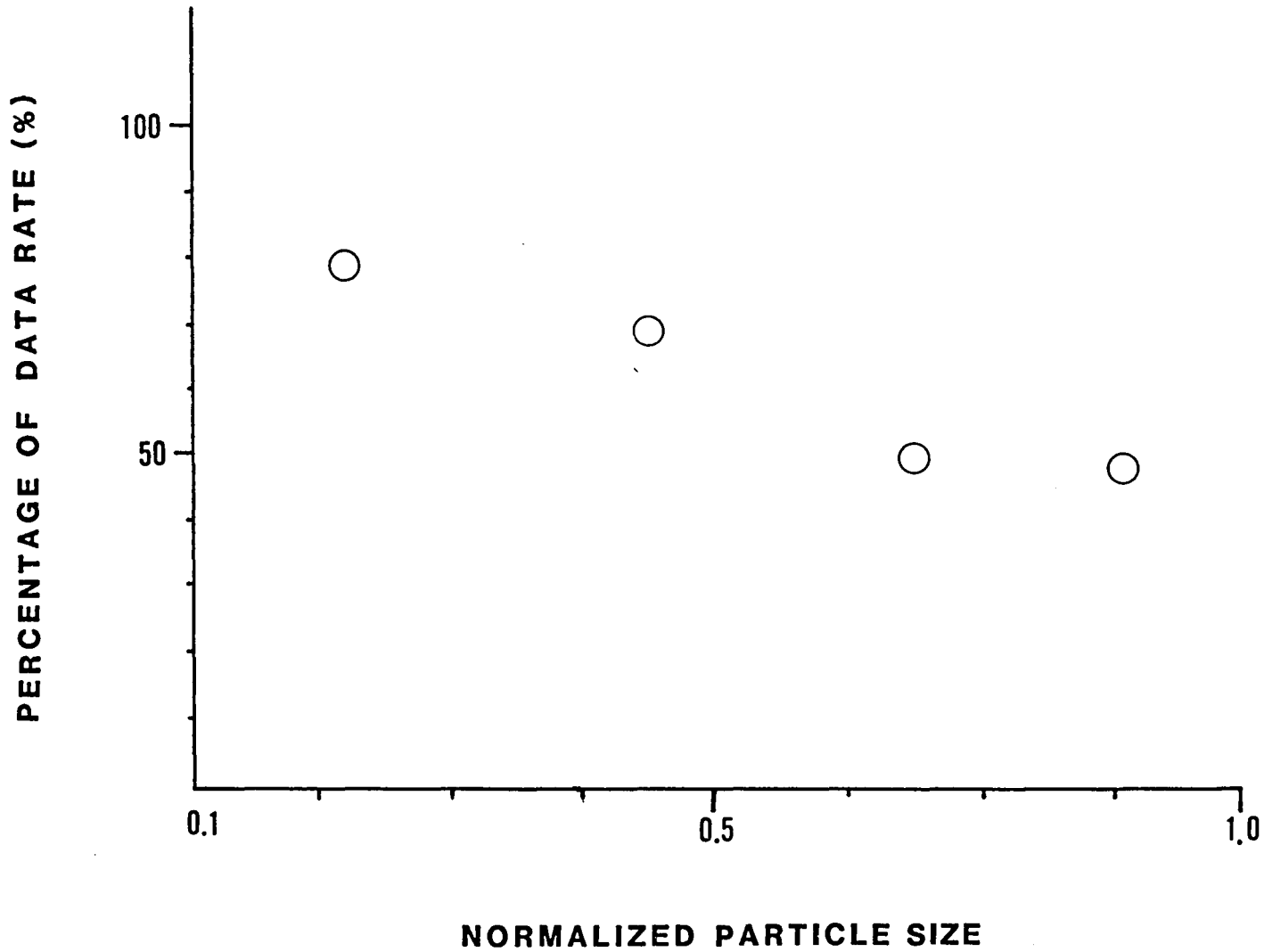
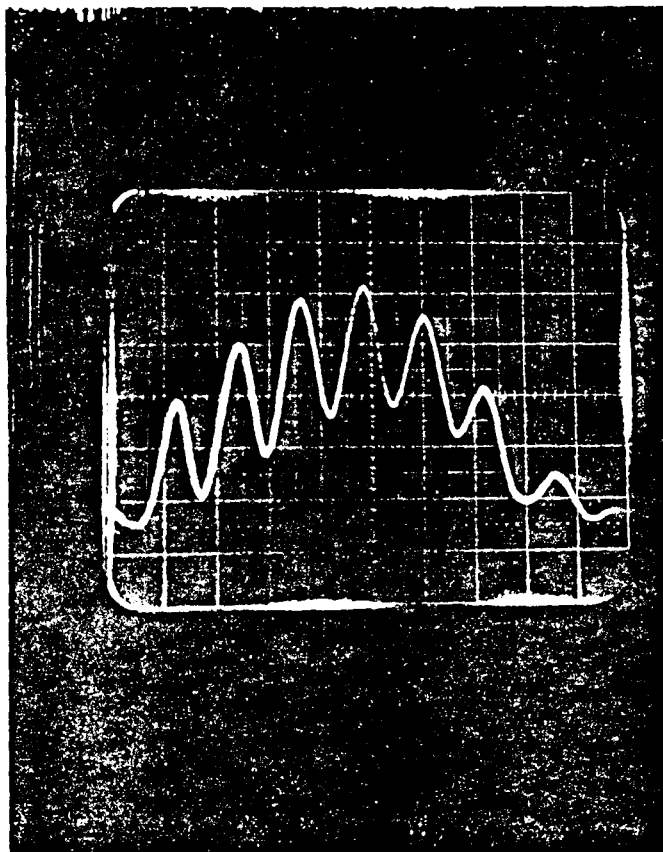


Figure 12. Effect of spray blockage on the data rate of collection as a function of particle size.

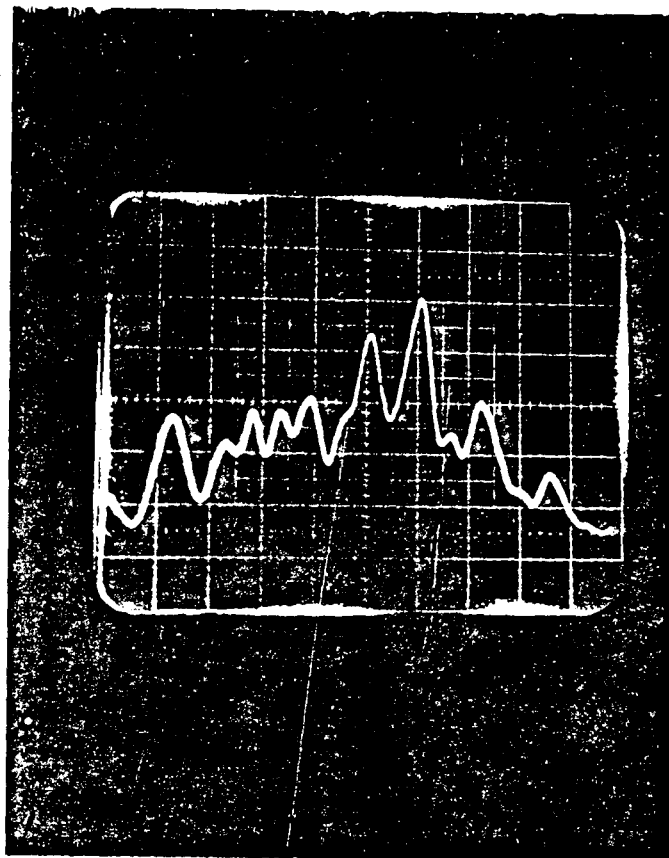
invariably the same, namely the large drops are more susceptible to rejection than the small drops. This effect can be corrected, or at least minimized, with proper electronics. Analyses of the signals with a storage oscilloscope showed that the large drops, since they have a low visibility, are more subject to the interference. A low visibility results in a low ac signal level. Present LDV processors base their acceptance criterion on the number of equal time crossings. Spray interference will introduce random crossings which disturb the otherwise periodic function. This is illustrated in Figures 13a and 13b which are photographs from the storage oscilloscope. This disturbance is less important for high visibility signals. In the actual rain, or simulated rain, experiments this effect will not be as pronounced since the LWC is typically two orders of magnitude smaller than the ones reported here. However, more sophisticated acceptance criteria will reduce considerably the errors due to the discrimination of the processor used in this work (VP1001). Therefore, even in the presence of extremely high interference the data rate should not change significantly.

Polydisperse Spray

A water spray produced by a pressure nozzle (Spray Systems Teejet TG10 at 4 psi) was measured with and without the additional interference introduced by the BURR 2. The results are shown on Figure 14. The most noticeable effect is the drop in data rate for the case with interference. As expected, the broadening is difficult to detect given that the measured distribution of sizes is broad to begin with.



(a)



(b)

Figure 13. Doppler signal of spherical droplet illuminated by (a) undisturbed laser beams; (b) laser beam traveling through rain spray. Scale for both pictures 0.1 ms/div and 1v/div.

COUNTS

-28-

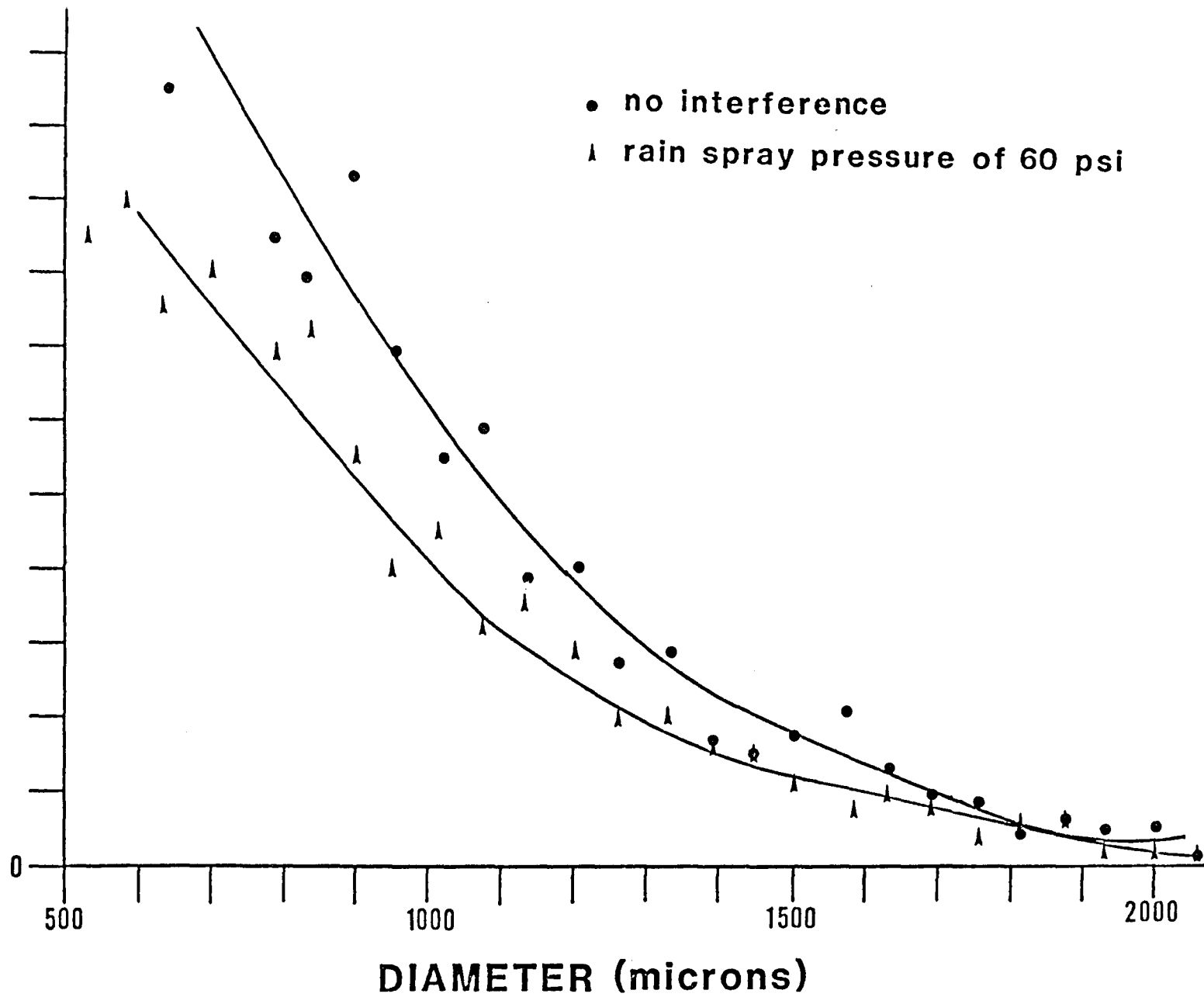


Figure 14. Size distribution of polydisperse spray with and without rain spray interference.

3.3 Measurements with 4 Mt. Receiving Optics

Rain spray measurements were also conducted with the receiver placed at 4.09 m from the probe volume and a collection angle $\theta = 20^\circ$. This was done to simulate the wind tunnel dimensions expected at NASA's facilities.

Based on previous spray measurements of this particular nozzle (BURR 2 single orifice) a size range of 600-6000 μm was chosen.

The system was calibrated with the 2800 μm droplets produced with the syringe-needle arrangement. Measurements were then made at the center of the spray ($z = 2.65$ m and $r = 0$) for nozzle pressures of 50, 60, and 70 psi.

Values of SMD and LMD for this particular size range are found to be within 10% of those corresponding to $f = 620$ mm $\theta = 90^\circ$. Table 2 shows the sauter mean and linear mean diameters for both receiving optics and the pressures of 50, 60, and 70 psi.

NOZZLE PRESSURE (psi)	SMD (μm)			LMD (μm)		
	$\theta=90^\circ$ f=620 mm	$\theta=20^\circ$ f=4090 mm	% discrep.	$\theta=90^\circ$ f=620 mm	$\theta=20^\circ$ f=4090 mm	% discrep.
50	1732	1931	11.5	1332	1440	8
60	1698	1846	9.0	1290	1260	2
70	1688	1624	4.0	1232	1276	4

TABLE 2

NOTE: SMD's and LMD's were computed in the 800-3000 μm size range common to both receiving optics.

4.0 THE EFFECT OF DROPLET ASPHERICITY IN THE SCATTERING SIGNAL

Slightly aspherical droplets were produced with the Berglund-Liu monodisperse generator. Droplets some distance from the vibrating orifice may be the result of the coalescence of two smaller droplets traveling at different speeds. These droplets will oscillate forming prolate and oblate spheroids. The stability and repeatability of this phenomenon are questionable. A strobe light triggered by a fraction of the frequency of the vibrating orifice permitted visual inspection of the droplets. The volume of the droplets is known since at any time the flow rate and number of droplets generated are known.

Receiving optics were positioned at 90° and 20° where the scattered light is primarily by reflection and refraction, respectively. The hypothesis was that the effect of shape would be more pronounced at 90° than at 20° since the scattering cross section of the latter is considerably larger. One consequence of using the Berglund-Liu is that the droplets are small (about $80 \mu\text{m}$) and therefore, don't scatter very much light, given that the sensitivity of the optics was set for much larger rain drops. This problem was alleviated by decreasing the probe volume to about $1.5 \text{ mm} \times 120 \mu\text{m}$ (obviously an argon-ion laser would solve this problem). Unfortunately, even with this reduced probe volume the S/N of the signals at 90° was low, and some of the broadening experienced in the size histogram is due to noise.

Figures 15a and 15b show the size histograms corresponding to spherical stable droplets at 20° and 90° , respectively. Figures 16a and 16b show equivalent measurements but the droplets are oscillating thus appearing as spheroids at the plane of measurement. It must be pointed

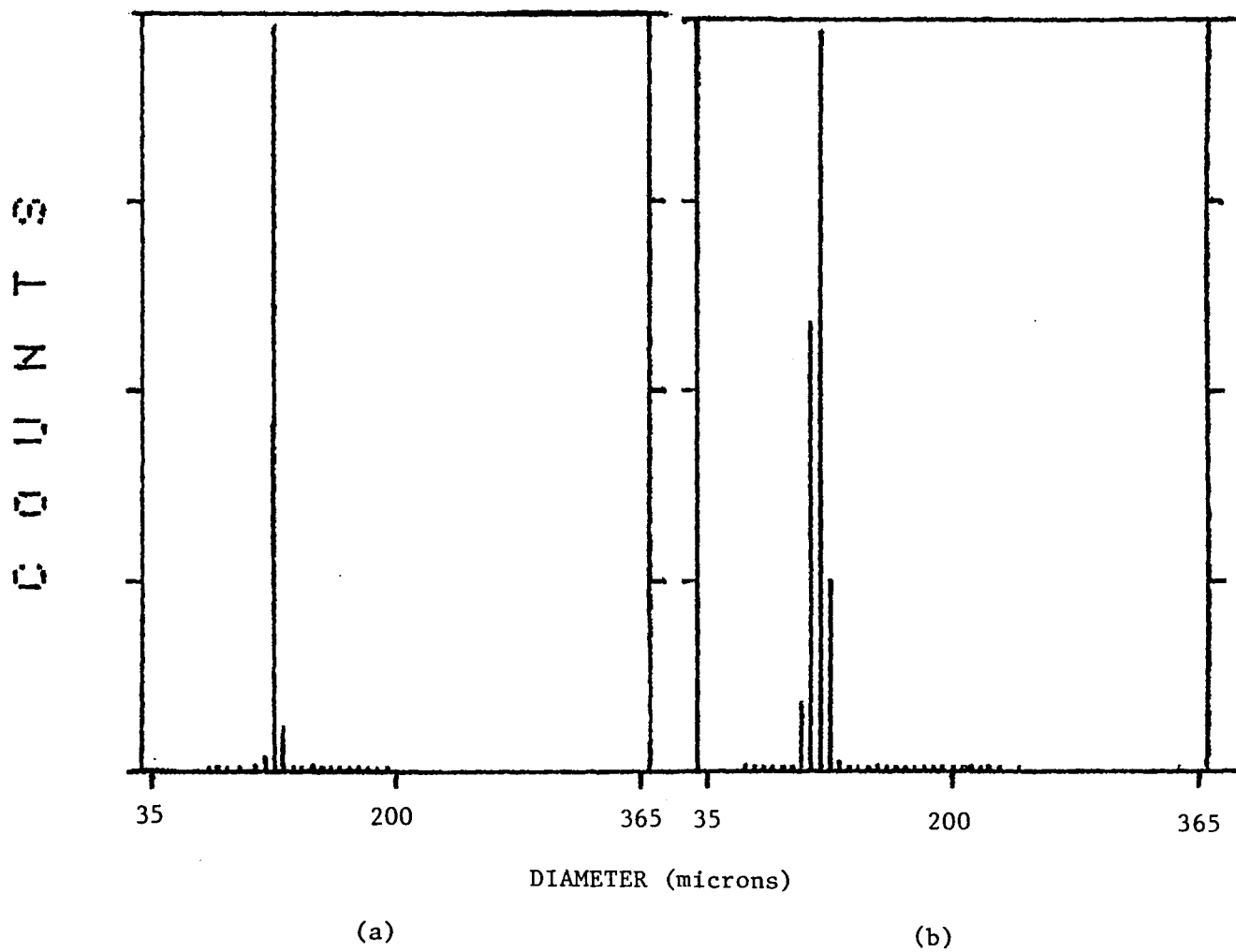


Figure 15. Size histogram of monodisperse spherical droplets collected at (a) 20° ; (b) 90° .

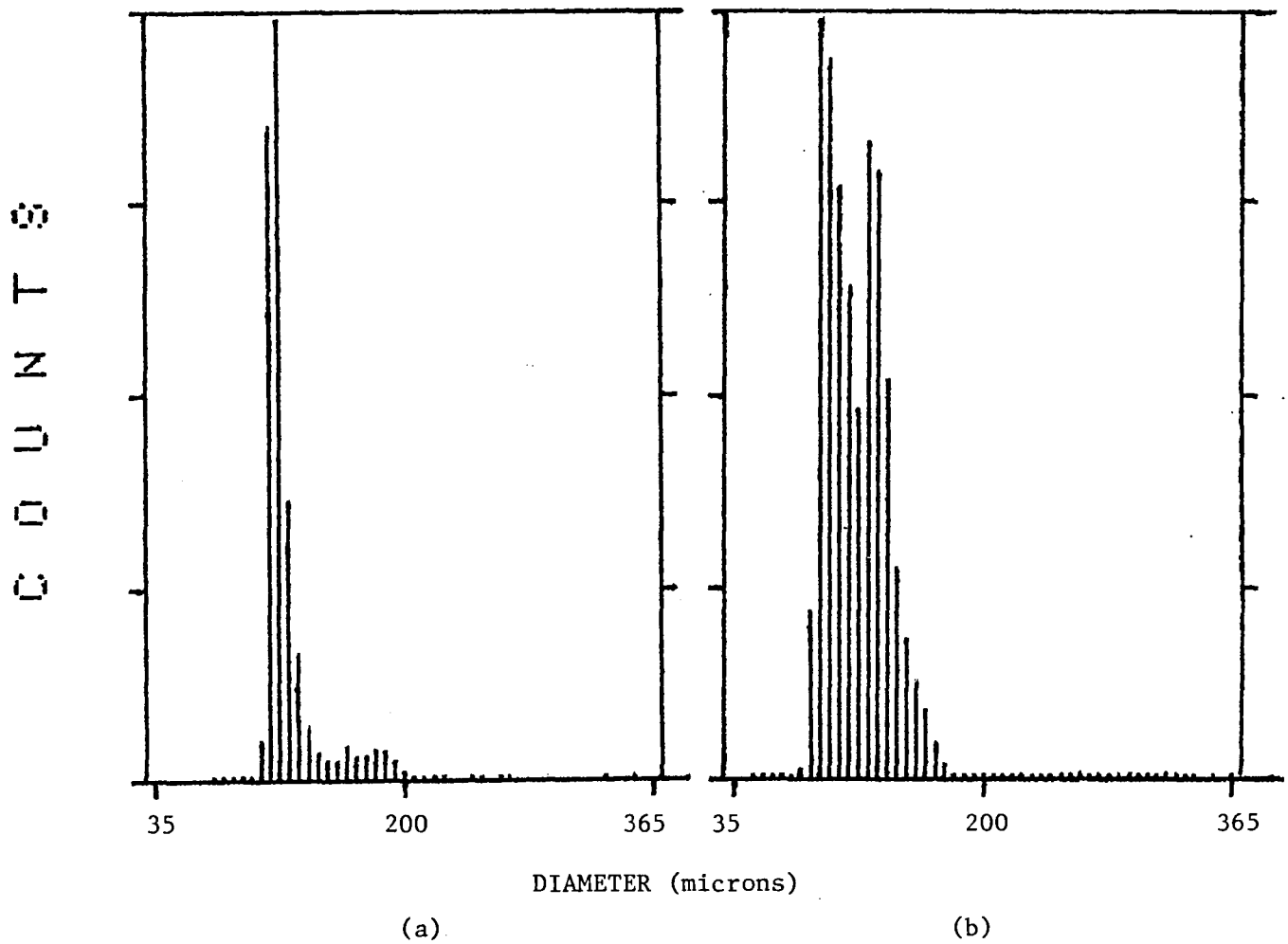


Figure 16. Size histogram of equal volume nonspherical droplets collected at (a) 20° ; (b) 90° .

out that with the aid of the strobe light we adjusted the frequency and position of the vibrating orifice to align the spheroids to the same direction at the plane of measurement. This, however, was not totally achieved and we might expect that different shape droplets (with the same volume) contributed to the histograms. Although the evidence is not solid, we are inclined to conclude that more broadening was experienced at 90° than at 20° .

In an effort to explain the effect of the droplet shape in the particle size, a very simple model was implemented. The model uses geometric scattering, therefore, dividing the scattered light into three components: reflection, refraction and diffraction. The model assumes that for a given angle of collection the scattered light due to either reflection or refraction is proportional to the illuminated area of the droplet. No regard is given to phase and interference since for the most part the light is collected over a finite solid angle. For angles of collection close to 90° the scattered light is primarily by reflection from the first surface of the droplet. Figure 17a shows that the laser beam travels along the y direction, and droplets of elliptical shape are moving down in the -z direction.

For an ellipsoid of revolution the cross section at the $z = 0$ plane is a circle of radius a. At the $y = 0$ plane the cross section is an ellipse with minor radius a and major radius b. If we place the receiving optics in the plane $z = 0$ and allow a finite solid angle of collection we get the following.

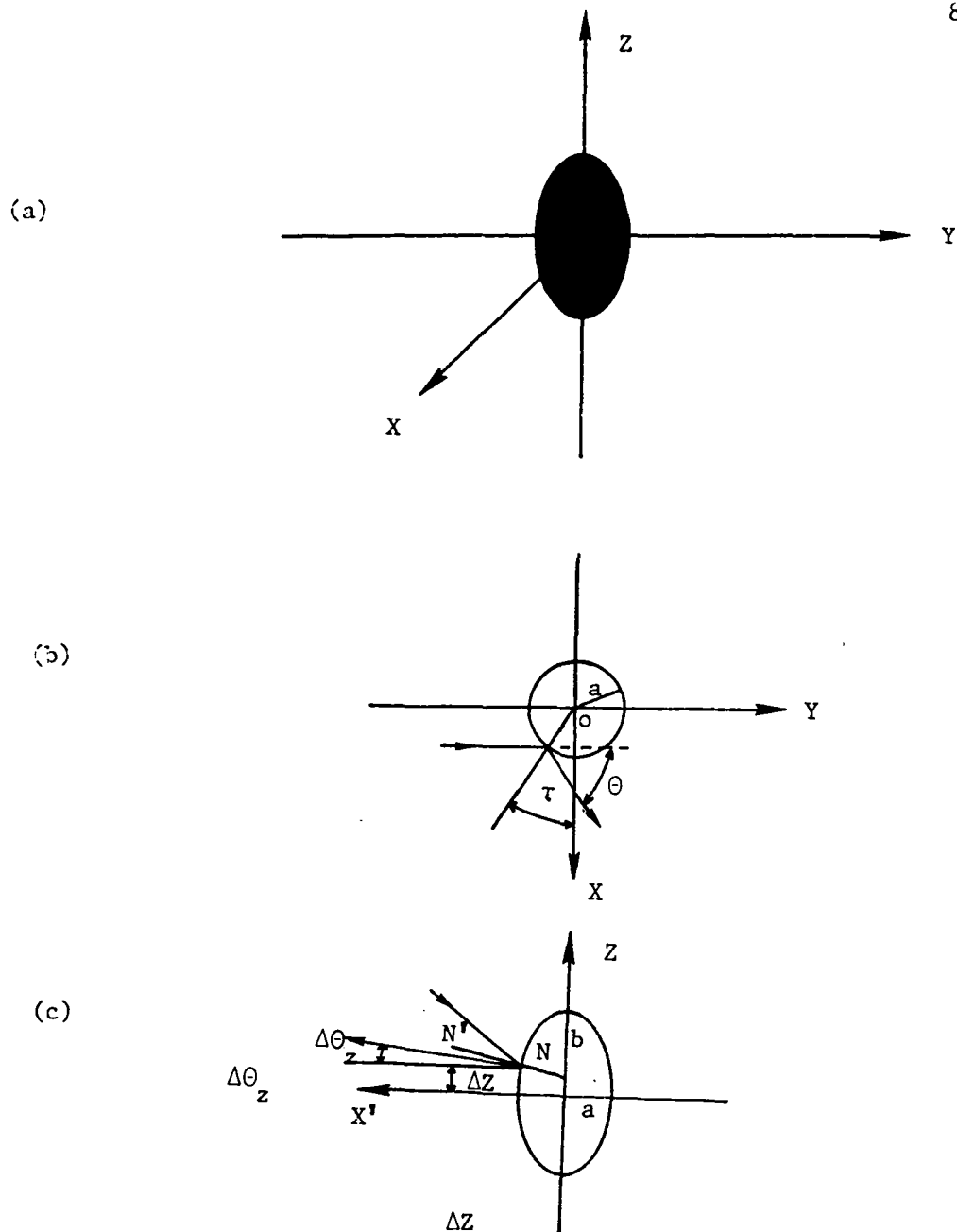


Figure 17. a) Coordinates of ellipsoid; b) Cross section of ellipsoid at $z = 0$; c) Cross section of ellipsoid at $y = 0$ after converting to x' y' coordinates.

For the $z = 0$ plane it can be shown that

$$\left| \tan \frac{\theta}{2} \right| = \frac{\sqrt{a^2 - x^2}}{x} \quad (x > 0)$$

where θ is the angle of collection solving for x :

$$x = a \cos \frac{\theta}{2}, \quad x > 0, \quad \theta < \pi \quad .$$

Since the receiving lens sustains a finite angle ($\Delta\theta$), there will be a finite Δx along the equatorial plane of the droplet, where

$$\Delta x = \left| \frac{a}{2} \sin \frac{\theta}{2} \cdot \Delta\theta \right| .$$

Similar calculations can be made along the ellipse described at $y = 0$. To simplify the mathematics the x and y axis are rotated by $-\tau$, such that the x axis is bisector of the incident and reflected beams. If we call this new coordinate x' , the ellipse at $y' = 0$ is given by (Figure 17b)

$$\frac{x'^2}{a^2} + \frac{z^2}{b^2} = 1 \quad .$$

The collection angle in the $x'z$ plane is $\Delta\theta_z$ which corresponds to half the angle sustained by the receiving optics around the equatorial plane. It can be shown that for small $\Delta\theta_z$

$$\Delta\theta_z \approx 2 \sin \frac{\theta}{2} \frac{a}{b} \frac{\Delta z}{\sqrt{b^2 - (\Delta z)^2}}$$

where Δz is the half width of the laser beam illuminating the ellipse on the $x'z$ plane such that the edge of this beam after reflection sustains a $\Delta\theta_z$ angle with the $x'y'$ plane. This yields at $\Delta z \ll b$

$$\Delta\theta_z \approx 2 \sin \frac{\theta}{2} \frac{a}{b^2} \Delta z \quad ,$$

therefore,

$$\Delta z = \frac{1}{2 \sin \frac{\theta}{2}} \frac{b^2}{a} \Delta\theta_z \quad .$$

For the assumptions listed above, the scattered light is proportional to $\Delta x \cdot \Delta z$. For a sphere of radius c ,

$$I_s \sim \left(\frac{c\Delta\theta}{2} \right)^2 R(\theta) \quad .$$

For the ellipsoid of radii a and b

$$I_s \sim \left(\frac{b\Delta\theta}{2} \right)^2 R(\theta)$$

where $R(\theta)$ is the reflectance of the droplet at a scattering angle θ .

It has been assumed that $\Delta\theta_z = \Delta\theta$ and $\cos(\Delta\theta_z) = 1$.

Volume conservation establishes that

$$c^3 = a^2 b .$$

Therefore, the ratio of the scattered light from a sphere to a prolate ellipsoid is:

$$\frac{I_{\text{sphere}}}{I_{\text{ell.}}} = \left(\frac{a}{b}\right)^{4/3} .$$

For instance Figures 15b and 16b show size histograms from stable spherical droplets and from oscillating spheroids of the same volume.

The ratio of the peak sizes $\left(\frac{d_{\text{min}}}{d_{\text{max}}}\right)$ indicated by the histograms is 0.75.

Based on the model it is then expected that the ratio of minor to major axis of the ellipse $\frac{a}{b} = \left(\frac{d_{\text{min}}}{d_{\text{max}}}\right)^{3/2} = 0.65$. Photographs taken in a different occasion show that $\frac{a}{b} = 0.63$.

A similar but more complicated analysis could be performed for the refracted light. Intuitively we feel that the error due to shape changes will be smaller when collecting refracted light.

5.0 REFERENCES

1. J. K. Luers, "Heavy Rain Effects on Aircraft," AIAA 21st Aerospace Sciences Meeting (1983).
2. V. Ramaswamy and P. Chýlek, "Shape of Raindrops" in Light Scattering by Irregularly Shaped Particles, ed. by D. W. Schuerman, P.55, Plenum Press (1980).
3. W. J. Humphreys, "Physics of the Air," McGraw-Hill (1940).
4. van de Hulst, "Light Scattering by Small Particles," Dover Publications, 1981.

1. Report No. NASA CR-177989		2. Government Accession No.		3. Recipient's Catalog No.	
4. Title and Subtitle Optical Technique to Study the Impact of Heavy Rain on Aircraft Performance				5. Report Date October 1985	
				6. Performing Organization Code	
7. Author(s) Cecil F. Hess and Funming Li				8. Performing Organization Report No. SDL 85-2424-1F	
9. Performing Organization Name and Address Spectron Development Laboratories, Inc. 3303 Harbor Blvd., Suite G-3 Costa Mesa, CA 92626				10. Work Unit No.	
				11. Contract or Grant No. NAS1-17932	
				13. Type of Report and Period Covered Contractor Report	
12. Sponsoring Agency Name and Address National Aeronautics and Space Administration Washington, DC 20546				14. Sponsoring Agency Code 324-01-00	
15. Supplementary Notes Langley Technical Monitor: R. Earl Dunham, Jr. SBIR Phase I - Final Report					
16. Abstract A laser-based technique was investigated and shown to have the potential to obtain measurements of the size and velocity of water droplets used in a wind tunnel to simulate rain. A theoretical model was developed which included some simple effects due to droplet nonsphericity. Parametric studies included the variation of collection distance (up to 4 m), angle of collection, effect of beam interference by the spray, and droplet shape. Accurate measurements were obtained under extremely high liquid water content and spray interference. The technique finds applications in the characterization of two phase flows where the size and velocity of particles are needed. Instruments based on this technique will find application in national laboratories, industry and universities.					
17. Key Words (Suggested by Author(s)) Particle sizing, laser velocimeter, raindrop sizing, two phase flows				18. Distribution Statement Unclassified - Unlimited Subject Category 35	
19. Security Classif. (of this report) Unclassified		20. Security Classif. (of this page) Unclassified		21. No. of Pages 42	22. Price* A03

End of Document